An Intricate Molecule: Aluminum Triiodide. Molecular Structure of AlI_3 and Al_2I_6 from Electron Diffraction and Computation

Magdolna Hargittai,* Balázs Réffy, and Mária Kolonits

Structural Chemistry Research Group of the Hungarian Academy of Sciences at Eötvös University, Pf. 32, H-1518 Budapest, Hungary

Received: November 9, 2005; In Final Form: December 20, 2005

The molecular structure of aluminum triiodide was investigated in the gas phase by high-temperature gas-phase electron diffraction and high-level computations. The geometries of monomeric, AlI_3, and dimeric, Al_2I_6, molecules were determined from two separate experiments carried out under carefully controlled conditions to prevent decomposition. This is the first experimental determination of the dimer structure by modern techniques. The computed geometrical parameters strongly depend on the applied methods and basis sets as well as on core-valence correlation effects. The electron diffraction thermal average bond length, r_g, of AlI_3 at 700 K is 2.448(6) Å; while those of Al_2I_6 at 430 K are 2.456(6) Å (terminal) and 2.670(8) Å (bridging). The equilibrium geometry of the monomer molecule is planar with D_{3h} symmetry. The dimer molecule is extremely floppy, and it is difficult to determine the symmetry of its equilibrium geometry by computation, as it is sensitive to the applied methods. MP2 and CCSD calculations find the Al_2I_6 molecule puckered with C_{2v} symmetry (although with a very small barrier at planarity), while density functional methods give a structure with a planar central ring of D_{2h} symmetry. Comparison of the computed vibrational frequencies with the gas-phase experimental ones favors the D_{2h} symmetry structure.

Introduction

Aluminum triiodide is an important and interesting compound. It has many practical applications in synthetic chemistry: it is used for cleaving epoxides[1] and esters;[2] it is a good carrier material for chemical transport reactions;[3,4] it forms complexes with many other metal halides and Lewis bases, either of the tetraiodo-aluminate, $MAlI_4$, type or the $AlI_3 \cdot DR_3$, donor−acceptor complex type. Recently, it has been shown that aluminum triiodide is a good starting material for the preparation of aluminum nitride, AlN, which is a ceramic material with excellent thermal conductivity and other outstanding properties.[5,6] Aluminum triiodide is a simple system. At the same time, its structure determination is apparently a difficult task as the rather diverse results in the literature indicate.

It has been recognized for a long time that the crystal structures of aluminum halides change from the fluorides toward the iodides. AlF_3 forms a 3D network of corner-sharing octahedra.[7] Aluminum is also six-coordinated in $AlCl_3$ but in a layer structure,[8] and aluminum tribromide has molecular crystals built up from dimeric Al_2Br_6 units, that is, the aluminum coordination changes here from six to four.[9,10,11] Wells[9] mentions that aluminum triiodide probably has a similar structure to that of aluminum tribromide, and Greenwood and Earnshaw[8] refer to it as a molecular crystal built from dimeric units. The first X-ray investigation of the aluminum triiodide crystal structure, however, found that the crystal consists of tetrahedral chains.[12] Two later studies, on the other hand, described the aluminum triiodide crystals to be molecular,[10,13] consisting of Al_2I_6 units. According to the latest investigation,[13] twinned crystals form during crystal growth, and it is difficult to find nontwinned pieces among them. Using twinned crystals could falsify the results of structure determination. Indeed, as we shall discuss later, the different crystal structure studies reported rather different geometrical parameters for aluminum triiodide.

Aluminum halides were among the first substances studied by gas-phase electron diffraction (GED) soon after the technique was developed.[14,15] Hedberg et al. carried out a GED study of aluminum triiodide recently as well.[16] In this latter work, the authors determined the structure of only the monomeric molecule because of dissociation of the dimer during heating, and the monomeric triiodide suffered a certain degree of decomposition as well. There have been numerous spectroscopic studies of aluminum triiodide: matrix isolation infrared (IR) spectroscopic study of the monomer,[17] an IR and Raman spectroscopic study of the melt,[18] a gas-phase Raman spectroscopic study,[19] and a gas-phase IR study[20] of both monomer and dimer. Perhaps due to the very large size of the iodine atom, the molecule had not yet been studied by high-level computational techniques; only a simple computation had been communicated together with the GED study of the monomer molecule.[16]

In this paper, we report the high-temperature electron diffraction and quantum chemical studies of both monomeric and dimeric forms of aluminum triiodide. We succeeded in getting diffraction pictures of both species in our electron diffraction study, and thus we could determine the geometrical parameters for both, from experiment as well as from computation.

Computations

The molecular structures of the aluminum triiodide monomer and dimer were calculated by ab initio (MP2, CCSD, CCSD(T), the latter only for the monomer) and density functional (B3LYP, B3PW91) methods. All computations were performed using the Gaussian03[21] program package. All-electron bases

10.1021/jp056498e CCC: $33.50
Published on Web 02/17/2006

TABLE 1: Computed Geometrical Parameters of AlI_3 and Al_2I_6[a]

basis[b]	iodine aluminum	SDB-TZ cc-pVDZ	SDB-TZ cc-pVTZ	SDB-QZ cc-pVTZ	SDB-QZ cc-pVQZ	DZ-PP cc-pVDZ	TZ-PP cc-pVTZ	TZ-PP cc-pwCVTZ	QZ-PP cc-pVQZ
				AlI_3					
Al−I	B3PW91	2.477	2.467	2.466	2.465	2.476	2.463		2.459
	MP2	2.476	2.460	2.457	2.458	2.474	2.447		2.433
	CCSD	2.484	2.467						
	CCSD(T)	2.486	2.469				2.457	2.451	2.442
	CCSD(T)FC1[c]						2.451	2.445	
	CCSD(T)full[d]						2.450	2.445	2.413
				Al_2I_6					
Al_1-I_5	B3PW91	2.494	2.483	2.483	2.483	2.491	2.481		2.477
	MP2	2.487[e]	2.473[e]	2.470[e]	2.465[e]	2.486[e]	2.460[e]		2.445[e]
		2.488[f]	2.473[f]	2.471[f]	2.465[f]	2.487[f]	2.461[f]		2.445[f]
	CCSD	2.497[e]	2.483[e]						
		2.498[f]	2.484[f]						
Δ_1[g]	B3PW91	0.017	0.016	0.017	0.018	0.015	0.018		0.018
	MP2	0.011	0.013	0.013	0.007	0.012	0.013		0.012
	CCSD	0.013	0.014						
Al_1-I_3	B3PW91	2.693	2.682	2.681	2.681	2.692	2.677		2.674
	MP2	2.689	2.667	2.666	2.658	2.688	2.650		2.632
	CCSD	2.703	2.679						
Δ_2[h]	B3PW91	0.199	0.199	0.198	0.198	0.201	0.196		0.197
	MP2	0.202	0.194	0.195	0.193	0.202	0.189		0.188
	CCSD	0.206	0.195						
$\angle I_5-Al_1-I_6$	B3PW91	120.0	120.1	120.0	120.1	120.5	120.1		120.0
	MP2	121.8	121.3	121.5	119.3	121.5	121.5		122.0
	CCSD	121.2	120.6						
$\angle I_3-Al_1-I_4$	B3PW91	94.3	94.7	94.6	94.1	94.5	94.7		94.7
	MP2	94.5	94.9	94.6	94.8	94.4	94.8		94.7
	CCSD	93.6	94.5						
$\angle\alpha$[i]	B3PW91	0.0	0.0	0.0	0.0	0.0	0.0		0.0
	MP2	28.6	26.9	28.7	27.8	25.3	27.8		32.0
	CCSD	20.5	16.3						

[a] Distances in Å, angles in deg. All calculations are frozen core, except where indicated otherwise. [b] For the description of bases, see the Computations section. [c] The next to largest noble gas core is frozen; that is, the outermost core orbitals are retained. [d] All electrons are included in the correlation calculation. [e] $Al-I_5$ distance. [f] $Al-I_6$ distance. [g] Difference of dimer terminal and monomer bond length. [h] Difference of dimer bridging and terminal bond length. [i] Puckering angle of the four-member ring, defined as the deviation of the angle between the two I_b-Al-I_b planes of the dimer from 180°.

were used for aluminum; the double-ζ (cc-pVDZ) (13s,9p,2d)/[5s,4p,2d], triple-ζ (cc-pVTZ) (15s,9p,2d,1f)/[5s,4p,2d,1f], and quadruple-ζ (cc-pVQZ) (16s,11p,3d,2f,1g)/[6s,5p,3d,2f,1g] bases of Woon and Dunnig.[22] For the monomer, the correlation consistent weighted core-valence triple-ζ (cc-p*w*CVTZ) basis of Peterson and Dunning[23] was also tested as it is recommended for calculating core-correlation effects on molecular properties. Quasirelativistic effective core potentials (ECP) and associated valence basis sets were used for iodine; they consider scalar relativistic effects, but not spin−orbit effects. A set of calculations was performed with a Stuttgart-type ECP published by Bergner et al.[24] containing 46 electrons ([Kr]4d^{10} "large core"). This potential was augmented by a triple-ζ (SDB-TZ) and a quadruple-ζ (SDB-QZ) valence basis set with a contraction scheme of (14s,10p,2d,1f)/[3s,3p,2d,1f] and (14s,10p,3d,2f,1g)/[4s,4p,3d,2f,1g], respectively. In other calculations, a "small core" scalar relativistic ECP[25] containing only 28 electrons ([Ar]-3d^{10}) was used for iodine, with larger correlation consistent valence electron bases,[25] triple-ζ (TZ-PP) (12s,11p,9d,1f)/[5s,-4p,3d,1f] and quadruple-ζ (QZ-PP) (14s,11p,12d,2f,1g)/[6s,5p,-4d,2f,1g]. For most calculations, the frozen core (FC) approximation was used, in which only the valence electrons are included in the correlation calculation.

We were also interested in the effect of electron correlation, and, in particular, of core-valence correlation, on the molecular geometry of the aluminum triiodide monomer. Therefore, a few calculations were carried out with the so-called "freeze inner noble gas core" option of Gaussian03, in which the next to largest noble gas core is frozen; that is, the outermost core orbitals are retained. Finally, a set of computations was also carried out in which all electrons, i.e., both core and valence electrons, were included in the correlation calculation.

The computed geometrical parameters of AlI_3 and Al_2I_6 are given in Table 1. From the two types of density functional (DFT) calculations, the B3PW91 results were much closer to the experimental values than the B3LYP ones; therefore, only the former are communicated. Frequency calculations were performed for all molecular species. According to expectation, monomeric aluminum triiodide is planar, and the calculated frequencies are in good agreement with the experimental ones; they are given in Table 2. We encountered some difficulties with the dimeric molecule. The density functional (B3LYP, B3PW91) methods found a D_{2h}-symmetry ground-state structure with a planar Al_2I_2 ring. At the same time, this geometry appears to be a transition state in the ab initio calculations (MP2, CCSD). These methods provide a C_{2v}-symmetry puckered molecule with a considerably bent four-membered ring as the ground-state structure. The two types of dimer structures are shown in Figure 1. The discrepancy is independent of the basis set. The computed frequencies of Al_2I_6, for both sets of computations, together with the gas-phase experimental values, are given in Table 3.

To get a realistic picture of the ground-state dimer structure, we calculated the potential energy surface around the minimum by different methods. It appears to be very flat and strongly method-dependent. The ground-state structure computed by ab initio methods (MP2 and CCSD) has C_{2v} symmetry, irrespective

TABLE 2: Experimental and Computed Vibrational Frequencies (in cm^{-1}) and Infrared Intensities (in km/mol, in Square Brackets) of AlI_3

			computed			
		exptl gas phase	B3PW91		MP2	
		ref 20	cc-pVTZ, TZ-PP	cc-pVQZ, QZ-PP	cc-pVTZ, TZ-PP	cc-pVQZ, QZ-PP
ν_1	A_1	156[a]	159.3	158.8	168.2	165.6
ν_2	A_2	147	143.5 [5.9]	144.4 [5.4]	151.2 [7.1]	152.6 [7.1]
ν_3	E	427	426.3 [128.5]	424.1 [127.4]	450.0 [135.5]	444.8 [138.1]
ν_4	E	66	63.4 [0.7]	63.9 [0.7]	65.8 [1.0]	66.4 [1.0]

[a] From ref 19.

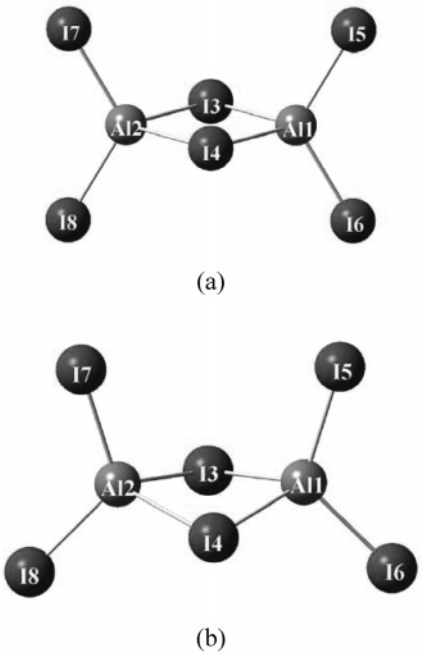

Figure 1. Molecular models of dimeric aluminum triiodide with (a) D_{2h} symmetry and (b) C_{2v} symmetry.

of the basis set. At the same time, the density functional methods, B3LYP and B3PW91, give the usual planar ring system as the ground-state structure (D_{2h} symmetry). We also calculated the puckering potential for the dimer molecule, together with the structural changes during puckering, to use it in a dynamical electron diffraction analysis (vide infra). The details are given in the Supporting Information.

Natural bond orbital (NBO) analyses were performed with the NBO program version 3.1,[26] implemented in Gaussian03. The so-called Wiberg bond indices were also calculated,[27] both are given in Table 4.

Normal Coordinate Analysis. A normal coordinate analysis was performed using the program ASYM20[28] for both monomeric and dimeric molecules. Vibrational amplitudes were calculated from the experimental[19,20] as well as from the computed vibrational frequencies (see Tables 2 and 3), and they are given in the Supporting Information. Generally, for a metal trihalide dimer, such as the Al_2I_6 molecule, the equilibrium structure has D_{2h} symmetry while the thermal average structure from GED has a puckered ring and thus C_{2v} symmetry. In this case, we had the peculiar situation that we had equilibrium structures (and thus frequencies) for both symmetries of the dimer from different computations. Therefore, we could calculate the vibrational amplitudes for both dimeric structures, D_{2h} and C_{2v}. They are rather different. For the GED analysis (referring to the thermal-average nature of the structure), the set of vibrational amplitudes calculated for the C_{2v} model was preferred and used as starting values in the analysis of the dimer structure.

Electron Diffraction Analysis. *Experiment.* The sample of aluminum triiodide was an Aldrich product. The electron diffraction patterns were recorded in the combined electron-diffraction/quadrupole mass-spectrometric experiment developed in the Budapest laboratory,[29] with a modified EG-100A apparatus and a radiation-type nozzle for the lower temperature experiment and a double-oven nozzle system for the higher temperature.[30] The nozzle material was molybdenum in both cases. The nozzle-tip temperature for the two sets of experiments was 435 and 700 K, respectively. It was known from the literature that it is difficult to get the dimer molecules into the vapor phase without decomposition. Thus, we made all efforts to use as low a temperature as possible. We used a larger than usual nozzle diameter and a larger than usual exposition time. For the monomer molecules, again, special care was needed. In the recent study of AlI_3,[16] the authors found that the monomer decomposed to a certain extent under their experimental conditions. Usually, with the double-oven technique the sample is placed in the colder part of the oven, which is heated to a temperature at which the dimer evaporates and through a connecting tube it gets into the second part of the nozzle, which is heated to higher temperature, at which the dimer dissociates. We experimented a great deal with the evaporation and found the following solution to be successful: the colder part of the nozzle, containing the sample, was not heated directly; only the second part was, and a shorter than usual stainless steal tube connected the two parts. Thus, the colder part of the nozzle was heated only by heat transfer. We used the quadrupole mass spectrometer to determine the temperature when the ions corresponding to the dimer molecule disappeared, and these were the experimental conditions under which we took the GED pictures. At this stage, the colder part was at 435 ± 10 K and the second part at 700 K.

Five and four and six and four photographic plates were used in the analyses of data taken at 50 and 19 cm camera ranges of the lower temperature (radiation nozzle) and higher temperature (double-oven) experiments, respectively. The data intervals were 2.00−14.00 Å^{-1} (with 0.125 Å^{-1} steps) and 9.00−25.00 Å^{-1} (with 0.25 Å^{-1} steps) at the two camera ranges, respectively. Electron scattering factors were taken from the literature.[31] Listings of electron diffraction molecular intensities are given in the Supporting Information. The molecular intensity and radial distribution curves are shown in Figures 2 and 3.

Analysis. In addition to the experimental difficulties (vide supra), a further difficulty is caused by the enormous scattering power of the iodine atoms compared to that of aluminum. This causes the molecular component of the scattered electron intensities to be much smaller than the atomic background, hence a poor signal/noise ratio with increasing scattering angles. For the lower-temperature experiment, that is the dimer structure,

TABLE 3: Experimental and Computed[a] Vibrational Frequencies (in cm^{-1}) and Infrared Intensities (in km/mol, in Square Brackets) of Al_2I_6

	D_{2h} model				C_{2v} model
symmetry	exptl, gas phase, ref 20	B3LYP	B3PW91	symmetry	MP2
A_g	339[b]	341.7	351.0	A_1	367.1 [8.9]
	145[c]	137.6	141.8	A_1	151.8 [0.1]
	93[c]	93.7	92.7	A_1	96.0 [<0.1]
	42[c]	38.9	38.3	A_1	41.0 [<0.1]
A_u		27.4	27.5	A_2	29.9
B_{1g}	408[b]	405.4	411.5	B_2	432.7 [17.9]
	63[c]	56.2	55.5	B_2	54.5 [0.7]
B_{2g}		169.2	188.4	A_2	202.6
	82[c]	79.5	78.8	A_2	80.3
B_{3g}	54[c]	48.3	47.9	B_1	47.9 [0.1]
B_{1u}	288	283.2 [69.5]	295.1 [66.6]	B_1	308.6 [71.0]
	64	58.5 [0.7]	59.0 [0.8]	B_2	63.8 [1.4]
B_{2u}	423	409.3 [194.4]	415.6 [197.7]	A_1	440.4 [186.8]
	75	73.5 [0.4]	72.8 [0.4]	A_1	77.2 [0.5]
		4.3 [0.1]	3.7 [0.1]	A_1	11.1 [0.1]
B_{3u}	315	307.4 [311.6]	317.0 [306.2]	B_2	329.3 [278.4]
	137	133.5 [8.6]	137.1 [6.9]	B_2	143.4 [6.3]
	64	60.9 [1.7]	59.9 [1.9]	B_1	68.0 [0.8]

[a] Basis sets: Al, cc-pVTZ; I, SDB-TZ. See Computations section for details. [b] Raman melt, from ref 18 (the 339 cm^{-1} symmetric stretching frequency was cited erroneously in ref 20). [c] Raman, gas-phase, ref 19.

TABLE 4: Partial Charges from NBO Analysis and Wiberg Indices for AlI_3, Al_2I_6, and AlF_3 Molecules[a]

	q (e)			Wiberg indices	
	B3PW91	MP2		B3PW91	MP2
			AlI_3		
Al	0.829	1.010	Al−I	1.023	0.971
I	−0.276	−0.337			
			Al_2I_6		
Al	0.685	0.825	Al_1-I_3	0.594	0.585
I_3	−0.141	−0.183	Al_1-I_5	1.002	0.969
I_5	−0.272	−0.319	Al_1-I_6	1.002	0.971
I_6	−0.272	−0.322			
			AlF_3		
Al	2.199	2.355	Al−F	0.481	0.396
F	−0.733	−0.785			

[a] Basis sets: Al, cc-pVTZ; I, SDB-TZ. See Computations section for details.

this fact is compounded by the canceling out of the molecular intensities at about $s = 27$ Å^{-1}, a typical phenomenon for molecules containing atoms with vastly different atomic numbers.[32] Thus, we encountered the strange situation that the intensity curve corresponding to the 19 cm camera range of the lower temperature experiment is of worse quality than the same of the higher temperature monomer experiment; it is noisy and diminishes much too early. It would only get stronger again around $s = 35$ Å^{-1}, which is outside the range of our equipment. This means that there are no good-quality intensity data at the larger scattering angles, which, in turn, would be important for a more reliable determination of bond lengths. After many trial refinements, we decided to dampen the contribution of the larger scattering angle intensities, above $s = 17.5$ Å^{-1}.

Monomer Experiment. First, we analyzed the data of the higher temperature experiment. Although on the basis of the quadrupole mass spectra taken at the same conditions, we hoped that there were only monomeric molecules in the vapor, we had to check the possible presence of both the dimer and the iodine molecule, the latter in case the monomer started to decompose. Apparently, this was the case with the previous experiment[16] that was carried out at a lower temperature than ours (note, however, that we used a different evaporation technique). For starting parameters we chose the monomer

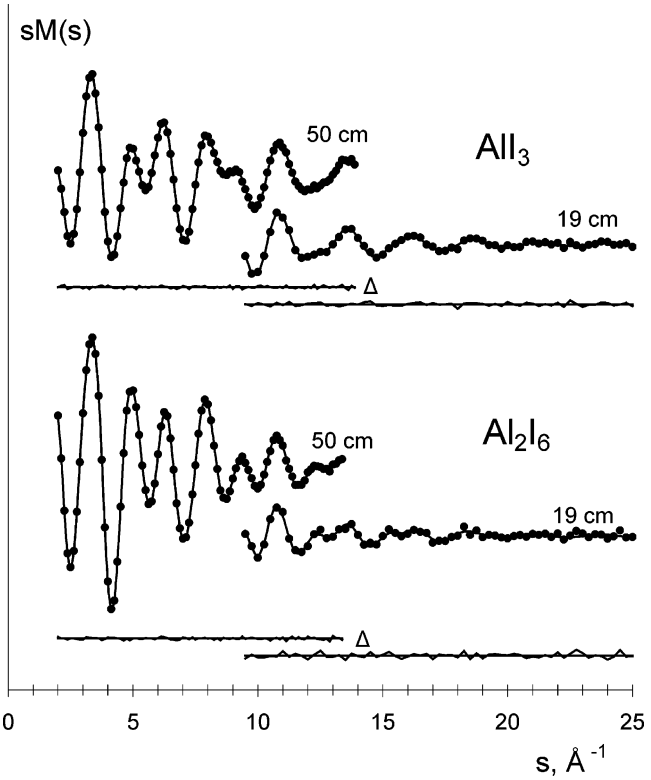

Figure 2. Experimental (dots) and calculated (solid line) molecular intensity curves and their differences for monomeric and dimeric aluminum triiodide.

distance of the previous study,[16] converted to our experimental temperature and the vibrational amplitudes calculated from the gas-phase experimental frequencies[20] for this temperature. Our analysis did not show any appreciable amount of either dimers or the iodine molecule to be present in the vapor phase.

Anharmonicity of the stretching vibrations has been shown to be important for metal halide molecules,[33] and we included the asymmetry parameter (κ), which takes the stretching anharmonicity into account. Refining this parameter gave $\kappa(\text{Al}-\text{I}) = 3.17 \times 10^{-5}$ Å^3, which corresponds to a reasonable Morse parameter of about 1.5 Å^{-1} (cf., for example, ref 34).

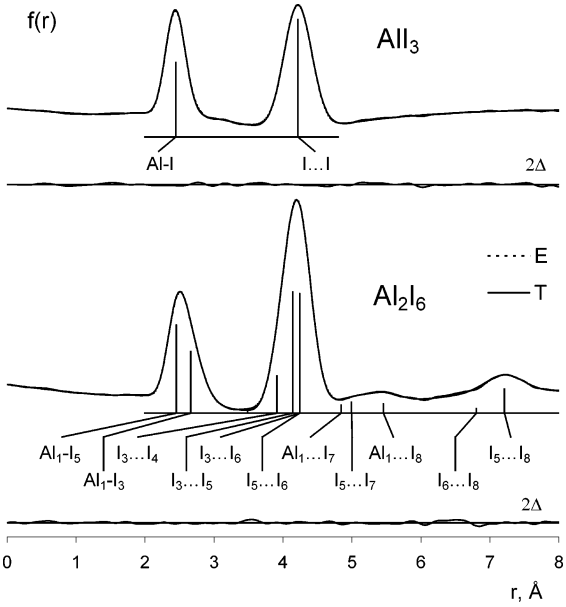

Figure 3. Experimental and calculated radial distributions and their differences (Δ, multiplied by 2) for AlI_3 and Al_2I_6.

At the same time, since this parameter influences the determined bond length, we also checked the impact of a different asymmetry parameter, calculated for a Morse parameter of 1.14 $Å^{-1}$. This Morse parameter was calculated from the spectroscopic parameters of the diatomic AlI molecule.[35] Although 1.14 $Å^{-1}$ seems to be somewhat low, the change was a mere 0.001 Å in the bond length, well within the experimental uncertainty.

According to previous experience, for a molecule with very large ligands connected to a small central atom even the nonbonded anharmonicity might be important.[36,37] Therefore, we included that parameter into our refinement as well. It turned out that the κ(I···I) value depended somewhat on how the background of the 50 cm camera-range intensity curve was drawn. As using the nonbonded asymmetry parameter was inconclusive, we ignored it in the final calculations. The only parameter that this assumption had influence on was the shrinkage of the monomer, but even that was within the experimental error. Nonetheless, we took this assumption into consideration when we calculated the final uncertainties. The geometrical parameters of monomeric AlI_3 from the GED experiment are given in Table 5.

Dimer Experiment. Due to the problems mentioned above, we had good-quality intensity data only in a relatively short range from the low-temperature experiment. There was strong correlation among various parameters; therefore, special precautions had to be taken during the structure analysis. First of all, we took into account the possible presence of monomeric molecules in the vapor. For doing so, we recalculated the Al−I bond length and the I···I nonbonded distance of AlI_3 for the lower temperature by proper vibrational corrections including anharmonicity from the high-temperature experiment. In the anharmonic correction we checked both Morse parameters used in the AlI_3 analysis. The vibrational amplitudes of the monomer were accepted from the normal coordinate analysis calculated for 435 K.

Further parameters taken from the computation, at least as starting values in the refinement, were the difference between the dimer terminal and bridging bond lengths, the terminal bond angle of the dimer, and the vibrational amplitudes of the dimer. The latter were calculated for both the D_{2h} and the C_{2v} symmetry structures. In modern GED structure analysis, it has become a standard to use the so-called "dynamic analysis" in which the large amplitude motion of the thermal average structure is described by a series of "conformers" calculated for gradually changing puckering angles. These structures were computed at the MP2 and B3PW91 level using Al, cc-pVTZ, and I, SDB-TZ, bases, and they are given in the Supporting Information. In this type of GED structure analysis, the differences of these "conformers" are taken from the computation as well as their contribution based on the calculated puckering potential. We tried this analysis in two different ways, based on the D_{2h} and C_{2v} equilibrium geometries, respectively. Interestingly, neither of these worked for this system, as the agreement between experimental and calculated intensities much worsened. The problem might be the larger than usual contribution of the longest nonbonded distances to the total molecular intensity distribution, due to the very large scattering power of the iodine atoms and the very small scattering power of aluminum. Thus, the approximation applied in the so-called dynamic analysis that is usually acceptable for systems with small ligands apparently does not work for such a system as the dimer of aluminum triiodide. Similarly, we did not find it realistic to do the GED analysis in the so-called "r_α" representation because of the unreliable perpendicular amplitudes (K) that the harmonic vibrational analysis provided. We calculated the latter for both the D_{2h} and the C_{2v} symmetry structures, with and without taking the smallest frequency values into account, but the very large scatter of the corresponding K parameters did not promise a reliable way of doing the refinement. Thus, we preferred the conventional, so-called static analysis.

There is another consequence of the larger than usual relative weight of the nonbonded distances in the scattering intensities. The goodness of fit (R factor), which is usually a good indication of the agreement between experimental and calculated intensities, was not that reliable here. We noticed during the structure analysis that a relatively good agreement could be reached with

TABLE 5: Geometrical Parameters of AlI_3 and Al_2I_6 from Electron Diffraction (from Separate Experiments)[a]

	r_g (Å), $\angle_a$ (deg)	l (Å)	κ (Å^3)
	Monomer		
r_g(Al−I)	2.448(6)	0.081(2)	3.2×10^{-5}(1.5×10^{-5})
r_e^M(Al−I)[b]	2.433(9)		
r_g(I···I)	4.224(10)	0.182(4)	
δ_g(I···I)[c]	0.016(4)		
δ_{calc}[d]	0.019		
	Dimer		
r_g(Al−I)$_t$[e]	2.456(6)	0.069(7)	1.6×10^{-5} [j]
r_e^M(Al−I)$_t$[b]	2.445(12)		
r_g(Al−I)$_b$[f]	2.670(8)	0.119(9)	1.5×10^{-4} [j]
r_e^M(Al−I)$_b$[b]	2.637(10)		
Δ_e(D_b−D_t)[g]	0.192(9)		
$\angle$(I_b−Al−I_b)	94.5(0.3)		
$\angle$(I_t−Al−I_t)	119.6(1.5)		
$\angle\alpha_a$[h]	30.8(4.0)		
$\angle\beta_a$[i]	3.0(2.0)		

[a] Error limits are estimated total errors, including systematic errors, and the effect of constraints used in the refinement $\sigma_t = (2\sigma_{LS}^2 + (cp)^2 + \Delta^2)^{1/2}$, where σ_{LS} is the standard deviation of the least squares refinement, p is the parameter, c is 0.002 for distances and 0.02 for amplitudes, and Δ is the effect of constraints. [b] Estimated experimental equilibrium distance, see text. [c] Experimental shrinkage: δ_g(I···I) = $\sqrt{3}r_g$(Al−I) − r_g(I···I). [d] Calculated shrinkage from normal coordinate analysis. [e] Terminal bond length of the dimer. [f] Bridging bond length of the dimer. [g] Difference of dimer bridging and terminal bond lengths, in r_e^M representation. [h] Puckering angle of the four-membered ring of the dimer; for definition see Table 1. [i] Tilt of the I_t−Al−I_t unit of the dimer. [j] Not refined.

many different bond angles and puckering angles because the respective nonbonded amplitudes together with the angles could refine the structure into one that gives acceptable agreement, and does that with acceptable values of these parameters. Nonetheless, when we calculated the radial distribution curve, we found a noticeable difference for many of these structures in the region corresponding to the bond lengths, which barely influenced the *R* factor. Thus, we could reach a relatively good agreement with a model that had about 8.5% monomers beside the dimer. However, for this model, the relative heights of the two main peaks of the calculated radial distribution did not fit their experimental counterparts, and this is due to the fact that in this model we "forced" too much monomer into the model, thus increasing the relative height of the first peak with respect to the second (the relative weight of the first peak is larger in the radial distribution of the monomer than on that of the dimer, see Figure 3). Thus, we believe that this model does not correspond to the experimental data. It is important to mention that the inclusion of this 8.5% monomer into the model changed the dimer bond lengths only by 0.001 Å, which is well within their experimental uncertainty.

The best agreement between experimental and calculated intensities was reached by a model that had no monomers. Its parameters are given in Table 5. In this case, all parameters could be refined, but due to the sometimes overwhelming correlation among the parameters, we carried out many trials with different parameters being constrained at the computed values. We could not fit any amount of either the monomer or the iodine molecule into any of these refinements.

Results and Discussion

The first GED study[14] on aluminum triiodide was reported in 1938 at the very beginning of the electron diffraction technique by the visual method, and the parameters determined for the dimer molecule, 2.53(4) and 2.58(4) Å for the two Al−I distances, are not realistic. The next experiment,[15] in the 1950s, was still done with the visual technique, and they determined the bond length of the monomer molecule at 2.44(2) Å, which, considering its large uncertainty, still holds. The latest investigation on aluminum trihalides by Hedberg et al.[16] reported a bond length (r_g) of 2.459(5) Å [in fact, the bond length is reported as r_g 2.459(5) Å in the abstract, r_g 2.461(5) Å in Table 8, and r_a 2.449(5), that would correspond to about 2.451 Å as r_g, in the Discussion section] for the monomer molecule at 573 K. There is thus some discrepancy with our r_g 2.448(6) Å value determined at about 700 K even though the difference is just at the edge of the experimental uncertainties (unless the r_a 2.449 Å is the correct one in ref 16, which would mean a good agreement with our results). Considering the nozzle-tip temperatures, our thermal-average distance should be slightly larger rather than smaller than that in ref 16. The description of the AlI_3 experiment in ref 16 conveys no information about the nozzle material and nozzle design. Apparently, there was a partial decomposition of the sample, which is indicated by the presence of about 8% iodine in the vapor. If some of the AlI_3 molecules decomposed, some of the aluminum monoiodide molecules might have also gotten into the vapor, and that might account for the longer bond determined for the AlI_3 molecule, since the Al−I bond length of the monoiodide is supposed to be somewhere between the bond lengths of I_2 and AlI_3.

Comparing the experimental bond lengths of monomeric aluminum and gallium trihalides from the fluorides to the iodides,[33] an interesting trend can be observed. For the GaF_3−AlF_3 pair, the bond length difference is about 0.09 Å (temperature effects are not considered here). This difference decreases toward the idodide; it is 0.05, 0.02, and 0.01 Å for the chloride, bromide, and iodide pairs, respectively. Thus, although aluminum is a much smaller element than gallium, their bond lengths in their iodides are very similar. The same observation holds for the comparison of the terminal $Ga-I_t$ and $Al-I_t$ bonds in the dimeric molecules. This shows that as the size of the ligand atoms increases, the van der Waals interaction between the halogen atoms becomes more and more a determining factor in the bond length. The partial charge on aluminum in the monomer is 1.01e (0.83e in the dimer), indicating that the bonding is highly covalent and the Al^{3+} description of the metal is not realistic. It is expected that the covalent character of the bonds increases toward the larger halogens. Indeed, the calculated Wiberg indices for AlI_3 and for the terminal $Al-I_t$ bond in Al_2I_6 are both 0.97, indicating that these are single covalent bonds, without much back-bonding from the iodine atoms. For comparison, the partial charge on Al in AlF_3 is 2.36e indicating a highly ionic bonding, in agreement with the 0.39 Wiberg index for the Al−F bond.

Aluminum triiodide is not an easy target for computation. Table 1 shows our computed geometries by different technique/basis set combinations. We estimated our "experimental" equilibrium bond length, r_e^M, of AlI_3 by applying anharmonic corrections[38] to be 2.433(9) Å. There is a (possibly fortuitous) perfect agreement with the MP2//QZ-PP/cc-pVQZ level computation (2.433 Å), but MP2 calculations have been shown to underestimate bond lengths. The agreement with the density functional results is poorer; even the best agreement there, with the B3PW91//QZ-PP/cc-pVQZ results, shows a difference of 0.026 Å. At the same time, the agreement between the experimental gas-phase and computed vibrational frequencies is very good for the DFT methods and is somewhat worse for the MP2 (see Table 2).

We also looked into the effect of electron correlation on the bond length of aluminum triiodide. For this we carried out a series of calculations at the CCSD(T) level, with three different basis set combinations. In each case, a small-core ECP of Peterson et al.[25] was used for iodine, with the associated bases sets of triple-ζ and quadruple-ζ quality with similar level all-electron basis sets on aluminum (see Table 1). For one set of computations, we used the so-called weighted core-valence basis set for aluminum as suggested in ref 23 for calculating core-correlation effects. For the triple-ζ calculations, we computed the bond length in three different ways: by a frozen core (FC) approximation, in which inner-shells are excluded from the correlation calculation; by a so-called "freeze inner noble gas core" (FC1) option of Gaussian03, in which the shell below the valence shell is also included in the correlation calculation; and, finally, with all electrons (both core and valence) correlated.

We found that the effect of core correlation on the bond length is rather large; the Al−I bond length decreases by 0.007 Å from the frozen core to the full correlation calculation at the triple-ζ level. The FC1 calculation gives a very similar result, a 0.006 Å decrease compared to the FC calculation, but this should not be surprising, since in our case the difference between the FC1 and the full correlation calculation is merely the two 1s electrons of aluminum. The use of the weighted core-valence basis set (cc-p*w*CVTZ) of Peterson and Dunning[23] for aluminum considerably improves the calculation at all levels; already at the FC level the shortening of the Al−I bond length is 0.006 Å compared to the use of the simple triple-ζ basis on aluminum. The change between the FC and full correlation for this set is about the same as for the triple-ζ case, 0.006 Å.

The effect of core correlation is even more pronounced at the quadruple-ζ level. The Al−I bond length of AlI_3 decreases by 0.03 Å from the FC to full CCSD(T) calculation (see Table 1), compared with the 0.007 Å decrease at the triple-ζ level. Peterson et al.[25] carried out FC CCSD(T) calculations on the iodine molecule and found a 0.016 Å decrease in its bond length in going from the triple-ζ to the quadruple-ζ basis, similar to what we found at the FC CCSD(T) level for AlI_3. Their I−I bond length decreased a further 0.005 Å in changing the basis from quadruple- to quintuple-ζ quality, thus indicating that the decrease was leveling off. We might expect a similar decrease of the Al−I bond length for the FC CCSD(T) calculation on going from quadruple- to quintuple-ζ quality. However, it is impossible to predict how much the Al−I bond length would decrease from the FC to the full CCSD(T) calculation at the quintuple-ζ level and then further on.

Spin−orbit effects were neglected in our calculations, and they might be expected to increase the bond length. The spin−orbit effect for the iodine molecule was calculated to cause an about 0.02 Å increase of the bond length.[39] The same effect for the HI molecule is about 0.003 Å.[40] Thus, we may expect an about 0.01−0.02 Å increase of the Al−I bond length due to the spin−orbit effect. If our full CCSD(T) quadruple-ζ bond length of 2.413 Å corresponded to the CBS limit, then with spin−orbit correction this would result in an about 2.43 Å equilibrium bond length, in agreement with our estimated experimental equilibrium bond length of 2.433(9) Å. However, it is quite likely that a better basis set would result in a further decrease and that would be too short even with spin−orbit correction, compared with the experiment. This is a topic for further study.

As to the dimer structures, there the most important question is the shape of the molecule, as the conclusion from the computations is not unambiguous. For such a dimeric molecule, we would expect a D_{2h} symmetry structure, with two halogen bridges forming a planar ring in the center (see Figure 1a), and this is what the density functional computations provided. The experimental spectroscopic results[18−20] were also interpreted by such a structure. At the same time, the D_{2h}-symmetry structure is a transition state at the MP2 and CCSD computational levels, and the ground-state structure appears to have a puckered central ring as shown in Figure 1b. These results are irrespective of the basis sets applied in the computations; they seem to be only method-dependent. The molecule is extremely floppy; it has 9 frequencies with values below 100 cm^{-1}, with the smallest puckering mode being about 4 cm^{-1} in the D_{2h} structure. Figure 4 shows the puckering potentials of the dimer by different methods. Apparently, the potential energy surface (PES) is very flat; the minimum of the C_{2v} structure is barely about 0.2 kcal/mol deeper than the D_{2h} barrier by the MP2 method and only by about 0.02 kcal/mol by the CCSD method. Conversely, puckering the planar ring even as much as 20−30° requires very small energy according to the DFT potential energy surface. Thus, the results probably suffer from the insensitivity of the computation to small details of the real PES, and it is impossible to distinguish between the two models. It is also worth mentioning that the MP2 method is known to overestimate the potential barriers of quasilinear and quasiplanar molecules. Comparison with the GED data cannot help in this respect as the thermal average structure of the dimer from electron diffraction would be puckered even if the equilibrium structure had a planar central ring. However, comparison of the experimental gas-phase vibrational spectra with the two sets of computed frequencies may give some guidance. Figure 5 shows

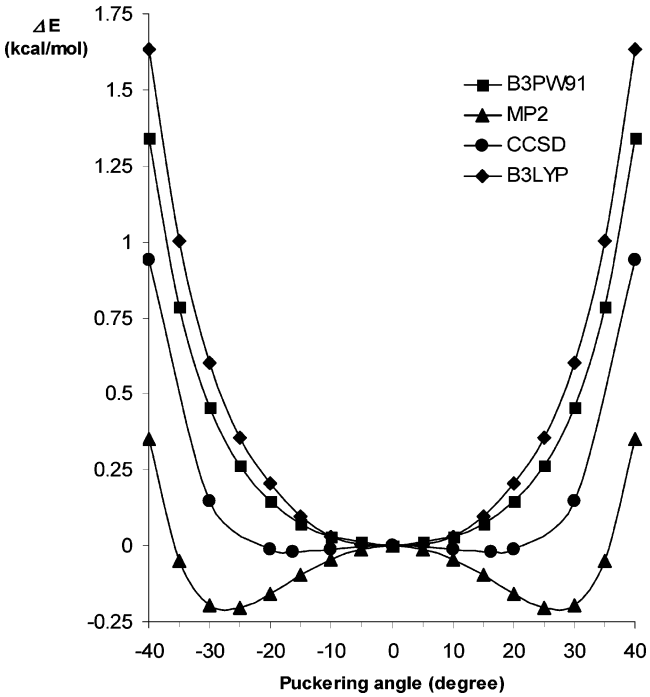

Figure 4. Puckering potential of the Al_2I_6 dimeric molecule from different levels of computation.

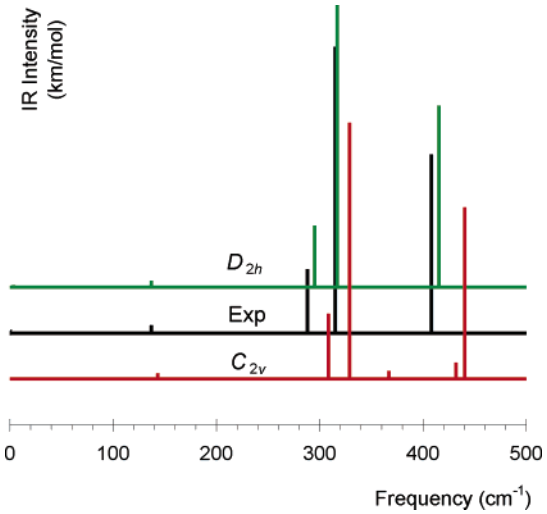

Figure 5. Vibrational spectrum of Al_2I_6 from experiment and computation (more spectral lines appear in the C_{2v} model than in the experiment).

the IR active modes of the vibrational spectrum for the experiment and the D_{2h} and C_{2v} structures, respectively. The shifts in the spectrum can be explained by the use of different computational methods as well as by the approximations applied in the computations, such as the harmonic approximation. Nonetheless, the fact that, due to the symmetry-lowering, there are more lines in the C_{2v} spectrum than in the D_{2h} one, and that these lines do not appear in the experiment, might be an indication that the aluminum triiodide dimer is planar, rather than puckered. We are inclined to believe that the puckered model resulting from the correlated ab initio calculations might just be a spurious effect.

Comparison of the monomer and dimer structures shows a pattern similar to other metal trihalides; the dimer terminal bond length from experiment is only slightly, by 0.012 Å, larger than the monomer bond length; referring to the estimated equilibrium distances, r_e^M. Different levels of computation give this difference in the range 0.01−0.02 Å. The difference of the two dimer

TABLE 6: Comparison of the Bond Lengths of Al_2I_6 in Crystalline and Vapor Phase

	crystal, ref 12	crystal, ref 10	crystal, ref 13	gas phase, this work[a]
Al−I_t	2.447(9)	2.48(2) [3×]	2.459(3) [2×]	2.441
	2.459(9)	2.49(2) [1×]	2.460(3) [2×]	
Al−I_b	2.703(9)	2.66(2) [2×]	2.656(3) [4×]	2.660
	2.738(9)	2.67(2)		
		2.62(2)		

[a] Calculated by the equation $r_\alpha = r_g - K - dr$, where K is the perpendicular amplitude, and dr is the centrifugal correction; the two latter are from a normal coordinate analysis in which the lowest frequency vibration is excluded.

bond lengths from GED is about 0.19 Å; again within the range of the computed differences (see Table 1). This parameter could be refined in the final stages of the structure analysis by GED, and the result, 0.192(9) Å, is in good agreement with the computations. The calculated Wiberg indices (see Table 4) are in agreement with these differences; while the monomer and the dimer terminal bonds have an about 1.0 bond order, the bridging bond's order is only about 0.5.

Aluminum triiodide has a molecular crystal containing dimeric units. As was discussed in the Introduction, its structure has been investigated repeatedly, and the results are quite different; apparently the crystal has the tendency to form twins, and that makes its structure determination complicated. Table 6 compares the two types of Al−I bond lengths from the X-ray diffraction studies and our gas-phase data (note that for this comparison the best representation is the r_α parameters corresponding to distances between average nuclear positions). For the terminal bond length there is a rather large scatter among the crystallographic data (about 0.04 Å), and our gas-phase bond length is smaller than any of the crystallographic ones. The agreement for the bridging bond is better; there, the scatter is only about 0.01 Å. Crystal packing effects, on the one hand, and the uncertainty in the correction of the GED thermal average parameters to r_α values, on the other, make this comparison of limited value.

Acknowledgment. This research has been supported by the Hungarian National Research Fund (OTKA T037978).

Supporting Information Available: Electron diffraction molecular intensities at two different camera ranges from both experiments; the computed puckering potential of the Al_2I_6 molecule and the computed geometrical differences between the differently puckered molecules; all bond lengths and nonbonded distances of the Al_2I_6 molecule, their experimental vibrational amplitudes, together with the calculated ones, the latter for both the D_{2h} and the C_{2v} models. This material is available free of charge via the Internet at http://pubs.acs.org.

References and Notes

(1) Eisch, J. J.; Liu, Z.-R.; Ma, X.; Zheng, G.-X. *J. Org. Chem.* **1992**, *57*, 5140.
(2) Mahajan, A. R.; Dutta, D. K.; Boruah, R. C.; Sandhu J. S. *Tetrahedron Lett.* **1990**, *31*, 3943.
(3) Oppermann, H.; Herrera, S.; Huong, D. Q. Z. *Naturforsch., B: Chem. Sci.* **1998**, *53*, 361.
(4) Schafer, H. *Z. Anorg. Allg. Chem.* **1975**, *414*, 151.
(5) Yoshioka, M.; Takahashi, N. Nakamura, T. *Mater. Chem. Phys.* **2004**, *86*, 74.
(6) Pouget, M.; Lecompte, J. P.; Billy, M. *J. Chim. Phys. Phys. Chim. Biol.* **1994**, *91*, 547.
(7) Lebail, A.; Fourquet, J. L.; Bentrup, U. *J. Solid State Chem.* **1992**, *100*, 151.
(8) Greenwood, N. N.; Earnshaw, A. *Chemistry of the Elements*, Pergamon Press: Oxford, 1984.
(9) Wells, A. F. *Structural Inorganic Chemistry*, 4th ed.; Clarendon Press: Oxford, 1975.
(10) Troyanov, S. I. *Zh. Neorg. Khim.* **1994**, *39*, 552.
(11) Berg, R. W.; Poulsen, F. W.; Nielsen, K. *Acta Chem. Scand.* **1997**, *51*, 442.
(12) Kniep, R.; Blees, P.; Poll, W. *Angew. Chem.* **1982**, *94*, 370.
(13) Troyanov, S. I.; Krahl, T.; Kemnitz, E. *Z. Kristallogr.* **2004**, *219*, 88.
(14) Palmer, K. J.; Elliott, N. *J. Am. Chem. Soc.* **1938**, *60*, 1852.
(15) Akishin, P. A.; Pambidi, N. G.; Zasorin, E. *Z. Kristallogr.* **1959**, *4*, 186.
(16) Aarset, K.; Shen, Q.; Thomassen, H.; Richardson, A. D.; Hedberg, K. *J. Phys. Chem. A.* **1999**, *103*, 1644.
(17) Perov, P. A.; Nedjak, S. V.; Maltsev, A. A. *Vesnt. Mosk. Univ.* **1974**, *2*, 201.
(18) Beattie, I. R.; Gilson, T.; Ozin, G. A. *J. Chem. Soc. A* **1968**, 813.
(19) Beattie, I. R.; Horder, J. R. *J. Chem. Soc. A* **1969**, 2655.
(20) Sjøgren, C. E.; Klaeboe, P.; Rytter, E. *Spectrochim. Acta* **1984**, *40A*, 457.
(21) Frisch, M. J.; Trucks, G. W.; Schlegel, H. B.; Scuseria, G. E.; Robb, M. A.; Cheeseman, J. R.; Montgomery, J. A., Jr.; Vreven, T.; Kudin, K. N.; Burant, J. C.; Millam, J. M.; Iyengar, S. S.; Tomasi, J.; Barone, V.; Mennucci, B.; Cossi, M.; Scalmani, G.; Rega, N.; Petersson, G. A.; Nakatsuji, H.; Hada, M.; Ehara, M.; Toyota, K.; Fukuda, R.; Hasegawa, J.; Ishida, M.; Nakajima, T.; Honda, Y.; Kitao, O.; Nakai, H.; Klene, M.; Li, X.; Knox, J. E.; Hratchian, H. P.; Cross, J. B.; Bakken, V.; Adamo, C.; Jaramillo, J.; Gomperts, R.; Stratmann, R. E.; Yazyev, O.; Austin, A. J.; Cammi, R.; Pomelli, C.; Ochterski, J. W.; Ayala, P. Y.; Morokuma, K.; Voth, G. A.; Salvador, P.; Dannenberg, J. J.; Zakrzewski, V. G.; Dapprich, S.; Daniels, A. D.; Strain, M. C.; Farkas, O.; Malick, D. K.; Rabuck, A. D.; Raghavachari, K.; Foresman, J. B.; Ortiz, J. V.; Cui, Q.; Baboul, A. G.; Clifford, S.; Cioslowski, J.; Stefanov, B. B.; Liu, G.; Liashenko, A.; Piskorz, P.; Komaromi, I.; Martin, R. L.; Fox, D. J.; Keith, T.; Al-Laham, M. A.; Peng, C. Y.; Nanayakkara, A.; Challacombe, M.; Gill, P. M. W.; Johnson, B.; Chen, W.; Wong, M. W.; Gonzalez, C.; Pople, J. A. *Gaussian 03*, revision B.05; Gaussian, Inc.: Wallingford, CT, 2004.
(22) Woon, D. E.; Dunning, T. H., Jr. *J. Chem. Phys.* **1993**, *98*, 1358.
(23) Peterson, K. A.; Dunning, T. H., Jr. *J. Chem. Phys.* **2002**, *117*, 10548.
(24) Bergner, A.; Dolg, M.; Kuechle, W.; Stoll, H.; Preuss, H. *Mol. Phys.* **1993**, *80*, 1431.
(25) Peterson, K. A.; Figgen, D.; Goll, E.; Stoll, H.; Dolg, M. *J. Chem. Phys.* **2003**, *119*, 11113.
(26) (a) Glendening, E. D.; Reed, A. E.; Carpenter, J. E.; Weinhold, F. NBO Version 3.1. (b) Carpenter, J. E.; Weinhold, F. *THEOCHEM* **1988**, *169*, 41. (c) Foster, J. P.; Weinhold, F. *J. Am. Chem. Soc.* **1980**, *102*, 7211. (d) Reed, A. E.; Weinhold, F. *J. Chem. Phys.* **1983**, *78*, 4066. (e) Reed, A. E.; Weinstock, R. B.; Weinhold, F. *J. Chem. Phys.* **1985**, *83*, 735. (f) Reed, A. E.; Curtiss, L. A.; Weinhold, F. *Chem. Rev.* **1988**, *88*, 899. (g) Reed, A. E.; Schleyer, P. v. R. *J. Am. Chem. Soc.* **1987**, *109*, 7362. (h) Reed, A. E.; Schleyer, P. v. R. *Inorg. Chem.* **1988**, *27*, 3969. (i) Weinhold, F.; Carpenter, J. E. *The Structure of Small Molecules and Ions*; Plenum Press: 1988; p 227.
(27) Wiberg, K. *Tetrahedron* **1968,** *24*, 1083.
(28) Hedberg, L.; Mills, I. M. *J. Mol. Spectrosc.* **1993**, *160*, 117.
(29) Hargittai, I.; Tremmel, J.; Kolonits, M. *HIS, Hung. Sci. Instrum.* **1980**, *50*, 31. Hargittai, I.; Bohatka, S.; Tremmel, J.; Berecz, I. *HIS, Hung. Sci. Instr.* **1980**, *50*, 51.
(30) Tremmel, J.; Hargittai, I. *J. Phys. E.* **1985**, *18*, 148.
(31) Ross, A. W.; Fink, M.; Hilderbrandt, R.; Wang, J.; Smith, V. H., Jr. In *International Tables for Crystallography*, *C*; Wilson, A. J. C., Ed.; Kluwer: Dordrecht, 1995; pp 245−338.
(32) (a) Seip, H. M.; Stølevik, R. *Acta Chem. Scand.* **1966**, *20*, 385. (b) Réffy, B.; Kolonits, M.; Schulz, A.; Klapötke, T. M.; Hargittai, M. *J. Am. Chem. Soc.* **2000**, *122*, 3127.
(33) Hargittai, M. *Chem. Rev.* **2000**, *100*, 2233.
(34) Hargittai, M.; Subbotina, N. Yu.; Kolonits, M.; Gershikov, A. G. *J. Chem. Phys.* **1991**, *94*, 7278.
(35) Wyse, F. C.; Gordy, W. *J. Chem. Phys.* **1972**, *56*, 2130.
(36) Kolonits, M.; Hargittai, M. *Struct. Chem.* **1998**, *9* (5), 349.
(37) Thomassen, H.; Hedberg, K. *J. Mol. Struct.* **1990**, *240*, 151.
(38) Kuchitsu, K. *Bull. Chem. Soc. Jpn.* **1967**, *40*, 505.
(39) Visscher, L.; Dyall, K. G. *J. Chem. Phys.* **1996**, *104*, 9040.
(40) Visscher, L.; Styszynski, J.; Nieuwpoort, W. C. *J. Chem. Phys.* **1996**, *105*, 1987.